



Facile synthesis of two-dimensional (2D) nanoporous NiO nanosheets from metal-organic frameworks with superior capacitive properties

Journal:	<i>New Journal of Chemistry</i>
Manuscript ID	NJ-CMT-08-2015-002261.R1
Article Type:	Letter
Date Submitted by the Author:	05-Nov-2015
Complete List of Authors:	<p>sun, zhipeng; a. Xinjiang University, Key Laboratory of Materials and Technology for Clean Energy, Ministry of Education, Key Laboratory of Advanced Functional Materials, Xinjiang University Urumqi, Xinjiang Province, CN; b.Xinjiang Uygur Autonomous Region Product Quality Supervision and Inspection Institute, 830011, China</p> <p>hui, lan; a. Xinjiang University, Key Laboratory of Materials and Technology for Clean Energy, Ministry of Education, Key Laboratory of Advanced Functional Materials, Xinjiang University Urumqi, Xinjiang Province, CN</p> <p>ran, wensheng; b.Xinjiang Uygur Autonomous Region Product Quality Supervision and Inspection Institute</p> <p>lu, yi; b.Xinjiang Uygur Autonomous Region Product Quality Supervision and Inspection Institute</p> <p>Jia, Dianzeng; Xinjiang University, Key Laboratory of Materials and Technology for Clean Energy, Ministry of Education, Key Laboratory of Advanced Functional Materials, Xinjiang University</p>



Journal Name

COMMUNICATION

Facile synthesis of two-dimensional (2D) nanoporous NiO nanosheets from metal-organic frameworks with superior capacitive properties

Received 00th January 20xx,
Accepted 00th January 20xx

DOI: 10.1039/x0xx00000x

Zhipeng Sun,^{a,b} Lan Hui,^a Wensheng Ran,^b Yi Lu,^b Dianzeng Jia^{*a}

www.rsc.org/

In this work, we demonstrate the design and fabrication of porous nickel oxide nanosheets (NiO NSs). The Ni-based intermediates (Ni(H₂O)₂[Ni(CN)₄]·XH₂O) are first prepared via an easy, environmentally friendly, and room temperature solution route. NiO NSs may well preserve morphology and then obtained by annealing treatment of Ni-based intermediates at 300 °C in air. Due to the high porous nanostructure, NiO NSs have a relatively high specific surface area of 118.2 m² g⁻¹. When evaluated for capacitive performance, the NiO NSs deliver a high specific capacitance of 527.1 F g⁻¹ at 1 A g⁻¹, and retain the good specific capacitance retention of about 80.2 % even at a high current density of 5 A g⁻¹ after 500 charge-discharge cycles.

With the awakening of ecological consciousness, people are searching for clean and green energy technologies to satisfy the ever-growing energy demand which, in principle, are also crucial for a sustainable world. Among various energy storage devices, supercapacitors (SCs), also known as electrochemical capacitors, have attracted considerable attention as hybrid power sources for electrical vehicles due to their higher power density, faster charging/discharging rates and longer lifespan than conventional batteries and capacitors.¹ As the performance of SCs mainly depends on the physical and chemical properties of the electrode materials, intense efforts have been focused on the research and development of the key materials.^{2,3} Up to date, various carbon-based materials have been widely explored as the electrode materials for SCs, owing to their high surface area, high conductivity, low cost and relative ease of preparation.⁴⁻⁷ Unfortunately, SCs using carbon-based materials are still far from satisfying the requirement of high capacitance since the dominant energy storage mechanism is charge separation. Recently, transition metal oxides have received intensive interests as the novel SC electrode materials because of their much higher

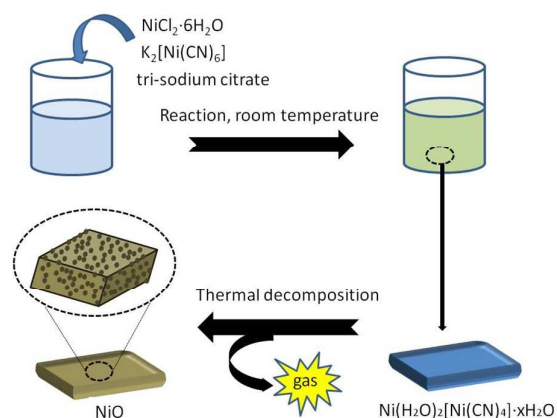
capacitance, which is based on the fast and reversible faradic redox reactions between the electrolyte and electrode.⁸ In addition, the development of nanostructured materials has been proposed to be a promising solution to greatly enhance their electrochemical performance by providing larger surface area for increasing the electrode/electrolyte contact area, and effectively shortening the transport path length of electron and ions.^{9,10} Moreover, the pores/cavities in the nanostructured materials can not only serve as the efficient ion reservoirs, but also facilitate the mass transport of electrodes within electrolytes, so as to further enhance their electrochemical performance.¹¹⁻¹³

Nickel oxide (NiO), a representative example of most used transition metal oxides, has been extensively studied as the electrode material for SCs in view of its high theoretical specific capacitance of 2584 F g⁻¹, high chemical and thermal stability, low cost, environment benign nature and easy preparation.^{14, 15} However, the specific capacitance of previous reported NiO nanostructures is far below its theoretical value, which might be attributed to the fact that the pseudocapacitance is mostly from the near-surface region of the electrode.¹⁶ To date, considerable efforts have been focused on developing novel porous NiO nanostructures that can greatly improve the supercapacitive performance.¹⁷⁻²¹ Unfortunately, these methods usually suffer from complex and time consuming synthesis procedures, resulting in low reproducibility and high cost. Therefore, it is of great importance to develop effective and facile methods to synthesize nanostructured NiO with rich porosity for high performance SCs. Metal-organic frameworks (MOFs), a new class of hybrid organic-inorganic supramolecular materials, have attracted great interest for a wide range of applications in catalysis, gas storage and sensing due to their high surface area and exceptional porosity.²² The presence of both organic and inorganic components enables easily tailoring the materials to achieve specific properties, such as pore size and surface chemical functionality.^{23,24} To this end, it would be natural to develop synthesis protocols and concepts by using MOFs as the precursor or template to fabricate porous nanostructured transition metal oxides for high performance SCs.

In this work, we report a simple room temperature solution method followed by convenient thermal annealing to fabricate nanoporous

Address: ^a Xinjiang University, Key Laboratory of Materials and Technology for Clean Energy, Ministry of Education, Key Laboratory of Advanced Functional Materials, Xinjiang University Urumqi, Xinjiang Province, 830046, China.
E-mail: zpsunxi@163.com; jdz@xju.edu.cn.

^b Xinjiang Uygur Autonomous Region Product Quality Supervision and Inspection Institute, 830011, China.



Scheme 1. Schematic illustration for the synthesis of NiO NSs.

NiO NSs with 2D nanostructures by utilizing a novel Ni-based metal organic framework (Ni-MOF; $\text{Ni}(\text{H}_2\text{O})_2[\text{Ni}(\text{CN})_4]\cdot\text{X}\cdot\text{H}_2\text{O}$) as precursors. A schematic illustration for the synthesis of porous NiO NSs is presented in Scheme 1. Ni-MOF precursors were firstly obtained by a simple solution reaction at room temperature, and then converted to NiO NSs via a mild thermal annealing without causing severe structural damage to their original state. Simultaneously, the porous structure could be readily produced due to the gas molecule release. Benefiting from the unusual nanostructure and relatively high specific surface area ($118.2 \text{ m}^2 \text{ g}^{-1}$), NiO NSs exhibit superior capacitive properties in terms of high specific capacitance (527.1 F g^{-1} at 1 A g^{-1}) and good cycling stability (500 cycles with 80.2 % retention at 5 A g^{-1}), which suggests its potential application in SCs. Ni-MOF precursors are first obtained from simple room temperature solution reaction, and their morphologies are characterized by FESEM and TEM (Figure 1). As seen in Figure 1a, Ni-MOF precursors show 2D nanosheet structures, many nanosheets are randomly aggregated over the entire area. A magnified FESEM image (Figure 1b) reveals that the obtained nanosheets appear to be composed of several stacked layers, and the size of the nanosheets ranged from 100–400 nm. From TEM

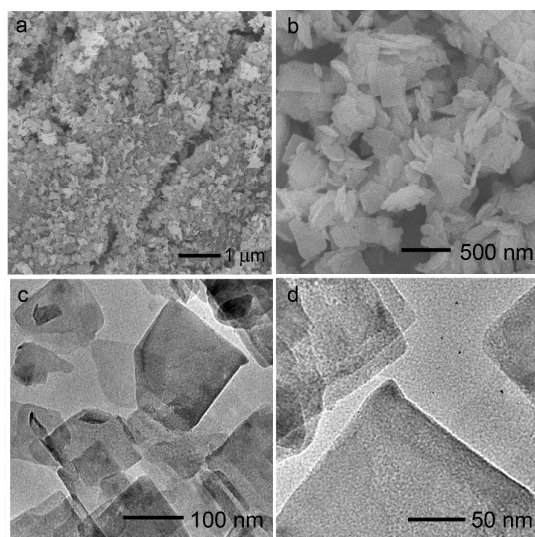


Figure 1 (a-b) FESEM images, (c-d) TEM images of Ni-MOF.

images (Figure 1c-d), Ni-MOF precursors display irregular shape, their solid and dense nature without discernible porosity. From the XRD pattern (Figure S1), all of the diffraction peaks can be assigned as an orthorhombic system, which matches the Hofmann-type $\text{Ni}(\text{H}_2\text{O})_2[\text{Ni}(\text{CN})_4]\cdot\text{X}\cdot\text{H}_2\text{O}$ with a 2D layered structure.²⁵ The Ni-MOF precursors were transformed into NiO NSs by annealing in air. As shown from Figure 2a, the sheet-like morphology may be perfectly maintained after the annealing process, and the thickness of nanosheet is estimated to be around 27 nm (Figure S2). As revealed by the magnified FESEM image (Figure 2b), the surface is relatively rough, and the porous nanosheet structure is perfectly constructed. In some areas, some small porous NiO NSs exist in these products, possibly indicating that large NiO NSs have been broken into those small nanosheets through the strong sonication process, as shown in the TEM images (Figure 2c-d). It is indicated that the morphology of NiO NSs is different from that of Ni-MOF precursors to some extent. The high magnified view (Figure 2e) indicates that these nanosheets are composed of quantities of NiO nanoparticles with size of 5–8 nm, in which the (200) crystal plane of NiO structure can be indentified with the interplanar distance of 0.209 nm.²¹ Importantly, a large number of small pores can be shown in the structure, which might be created by the evaporation of coordinated water molecules at the interlayer space in Hofmann analogue Ni-MOF precursors after the thermal annealing. Moreover, a typical XRD pattern of Ni-MOF precursors after calcinations is further demonstrated in Figure 2f, all the identified peaks can be assigned to the cubic phase of NiO (JCPDS file no. 4-835, space group: $Fm\bar{3}m$). No impurity phases were observed. It is further confirming that NiO NSs were formed after the annealing of Ni-MOF precursors at 300°C for 1 h. As predicted, the strikingly specific surface area of NiO NSs of $118.2 \text{ m}^2 \text{ g}^{-1}$ is verified from the BET result, possibly owing to the existence of nanopores (Figure S3a, b).

We further study the morphologies via slightly modifying the experimental parameters. The effect of DTC concentration on the structure of the products is firstly investigated. Figure S4a shows Ni-MOF precursors prepared with the addition of 1 mmol DTC. The obtained products display irregular sheet-like structure, but most of these nanosheets with the front size of 50–100 nm are no uniform and stacked together heavily. On the other hand, when the amount of DTC is increased to high concentration (4 mmol), the obtained products almost exhibit hexagon sheet-like structure with the front size of 200–250 nm and the average thickness of about 70 nm (Figure S4b). Moreover, a series of time-dependent processes for Ni-MOF growth is also conducted, from which we can gain more insight into the evolution process. From the SEM images (Figure S5), Ni-MOF with similar morphologies and nanostructures can be achieved in different stages. However, the generation of product yield will be enhanced with increasing of the time-dependent processes (Figure S6). From the above results, the roles of DTC and reaction time might be summarized. The DTC plays an important in organizing the overall structure of the obtained product. By changing its concentration, the products could be facily tuned to be 2D nanosheets with hexagonal pyramid shape. Additionally, the morphology of Ni-MOF precursors is not changed with increasing of the time-dependent processes except for improving the product yield.

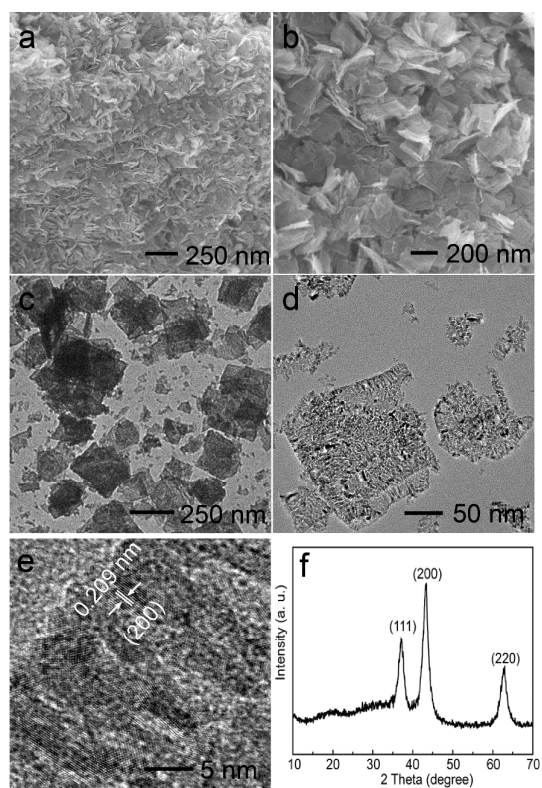
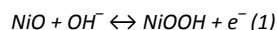


Figure 2 (a-b) FESEM images, (c-e) TEM images, and (f) XRD pattern of NiO NSs.

We further study the electrochemical properties of NiO NSs as the electrode material for SCs. The representative CV curves of NiO NSs at different scan rates of 1, 3, 5, 10 and 30 mV s^{-1} are shown in Figure 3a. It can be seen that a distinct pair of redox peaks during the anodic and cathodic sweeps, whose intensity increases clearly with the scan rate. It can be attributed to the following reversible reaction:²⁶



Indicating that the pseudocapacitive characteristic of NiO NSs. Based on the CV measurements, the specific capacitances of the samples were calculated using the following equation:²⁷

$$C = \frac{1}{mv(V_f - V_i)} \times \int_{V_i}^{V_f} I(V) dV \quad (2)$$

Where m is the mass of the active material, v is the scan rate, V_i and V_f are the potential limits of the voltammetric curve, and $I(V)$ is the instantaneous current. The calculated specific capacitance of NiO NSs (Figure 3b) is about 694.4, 540.1, 509.3, 463.0 and 331.8 F g^{-1} at scan rates of 1, 3, 5, 10 and 30 mV s^{-1} , respectively.

Figure 3c displays galvanostatic discharge curves of NiO NSs at different current densities. As can be seen, a distinct plateau can be observed in every curve, corresponding to the forward reaction in Equation (1). The specific capacitances were also evaluated from the galvanostatic charge/discharge tests. Based on discharge curves,

the capacitances of the samples were calculated as follows:²⁷

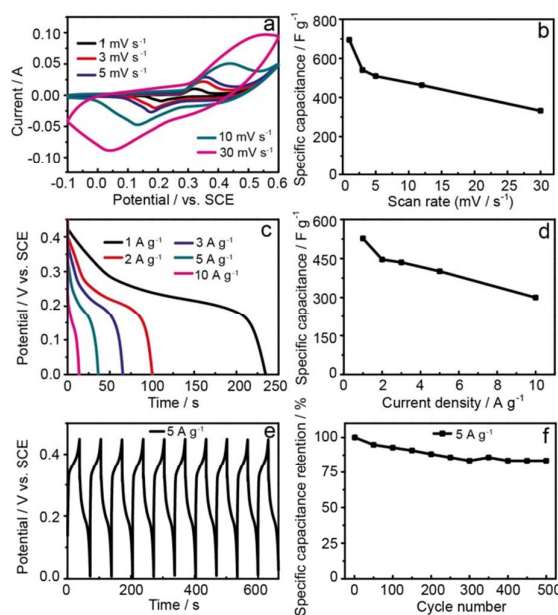


Figure 3 Electrochemical characterizations of NiO NSs: (a) CV curves at various scan rates; (b) Average specific capacitance at various scan rates; (c) Galvanostatic discharge curves at various discharge current densities; (d) Specific capacitance at various discharge current densities; (e) Galvanostatic charge and discharge voltage profiles at 5 A g^{-1} ; (f) Comparative cycling performance of different samples at 5 A g^{-1} .

$$C = (I \times \Delta t) / (\Delta V \times m) \quad (3)$$

Where I is the constant discharge current, Δt is the discharge time, m is the mass of active materials, and ΔV is the potential drop during discharge. The specific capacitance for NiO NSs are about 527.1, 446.2, 435.3, 401.1 and 300.0 F g^{-1} at different current densities of 1, 2, 3, 5 and 10 A g^{-1} , respectively (Figure 3d). Remarkably, about 56.9% of capacitance is retained when the current density increases from 1 to 10 A g^{-1} , indicating that NiO NSs have good high-rate discharge ability. Figure 3e shows the charge/discharge voltage profiles of the first 10 cycles, the coulombic efficiency is nearly 98.9% for each cycle of charge and discharge. Cycling stability is another important performance indicator for SCs. To examine the cycling stability of NiO NSs, constant current (5 A g^{-1}) charge-discharge cycling tests were carried out. As shown in Figure 3f, ~83.5% of the specific capacitance retention is retained after 500 cycles. Here NiO NSs exhibit better electrochemical characteristics than that of recent literatures (see Table 1), making it potentially useful for improved supercapacitor materials. Measured by the same CV or galvanostatic method in similar systems, the good capacitive performance of NiO NSs might be attributed to the high surface area and structural features including nanoheet assembly and void space, granting good accessibility through the electrolyte to the active material.²⁸ Moreover, the 2D nanosheet nanostructure could enable efficient transport of electrons.²⁹

In summary, 2D NiO NSs are fabricated by a simple room-temperature solution method and convenient thermal annealing using a novel Ni-MOF as precursors. Because of the nanoporous interior and 2D structure, these NiO NSs have a relatively high specific surface area. When evaluated for supercapacitive performance, NiO NSs demonstrate good performance with a high capacitance of 527.1 F g^{-1} at 1 A g^{-1} , which suggests that these NiO NSs are very promising for high performance SCs.

Acknowledgements

This project is supported by Thousand Talents Plan Xinjiang project, and Technology Foundation for Selected Overseas Chinese Scholar, Ministry of Personnel of China.

Experimental

Nickel (II) chloride hexahydrate ($\text{NiCl}_2 \cdot 6\text{H}_2\text{O}$, 98%, Sigma-Aldrich), $\text{K}_2[\text{Ni}(\text{CN})_6]$ (99.9%, Aldrich), dehydrate tri-sodium citrate (DTC) (99.0%, Sigma-Aldrich). In a typical procedure, 4 mmol of $\text{NiCl}_2 \cdot 6\text{H}_2\text{O}$ and 3 mmol of DTC are dissolved in 200 mL deionized water and stirred for 5 min. Then the solution is mixed with a $\text{K}_2[\text{Ni}(\text{CN})_6]$ aqueous solution that is made by dissolving 4 mmol $\text{K}_2[\text{Ni}(\text{CN})_6]$ into 200 mL deionized water. The mixture is aged at room temperature for 0.5 h. The product is collected by centrifugation (10000 rpm) and washed with deionized water several times. The product is then dried, followed by annealing at 300°C (heating rate 1°C min^{-1}) for 1 h to get NiO NSs.

Notes and references

- [1] F. Béguin, V. Presser, A. Balducci and E. Frackowiak, *Adv. Mater.* 2014, **26**, 2219.
- [2] J. R. Miller and P. Simon, *Science* 2008, **321**, 651.
- [3] W. Ai, W. Zhou, Z. Du, Y. Du, H. Zhang, X. Jia, L. Xie, M. Yi and T. Yu, W. Huang, *J. Mater. Chem.* 2012, **22**, 23439.
- [4] Z. Y. Jin, A. H. Lu, Y. Y. Xu, J. T. Zhang and W. C. Li, *Adv. Mater.* 2014, **26**, 3700.
- [5] Z. Laušević, P. Y. Apel, J. B. Krstić and I. V. Blonskaya, *Carbon* 2013, **64**, 456.
- [6] M. Yu, Y. Zhang, Y. Zeng, M. S. Balogun, K. Mai, Z. Zhang, X. Lu and Y. Tong, *Adv. Mater.* 2014, **26**, 4724.
- [7] W. Ai, X. Cao, Z. Sun, J. Jiang, Z. Du, L. Xie, Y. Wang, X. Wang, H. Zhang, W. Huang and T. Yu, *J. Mater. Chem. A* 2014, **2**, 12924.
- [8] G. Zhang and X. W. Lou, *Adv. Mater.* 2013, **25**, 976.
- [9] A. S. Arico, P. Bruce, B. Scrosati, J.-M. Tarascon and W. van Schalkwijk, *Nat. Mater.* 2005, **4**, 366.
- [10] X. Lu, T. Zhai, X. Zhang, Y. Shen, L. Yuan, B. Hu, L. Gong, J. Chen, Y. Gao, J. Zhou, Y. Tong and Z. L. Wang, *Adv. Mater.* 2012, **24**, 938.
- [11] X. Lu, T. Zhai, X. Zhang, Y. Shen, L. Yuan, B. Hu, L. Gong, J. Chen, Y. Gao, J. Zhou, Y. Tong and Z. L. Wang, *Adv. Mater.* 2012, **24**, 938.
- [12] J. Liu, J. Jiang, C. Cheng, H. Li, J. Zhang, H. Gong and H. J. Fan, *Adv. Mater.* 2011, **23**, 2076.
- [13] W. Ai, Z. Du, Z. Fan, J. Jiang, Y. Wang, H. Zhang, L. Xie, W. Huang and T. Yu, *Carbon* 2014, **76**, 148.
- [14] M. S. Wu, Y. A. Huang, J. J. Jow, W. D. Yang, C. Y. Hsieh and H. M. Tsai, *Int. J. Hydrogen Energy* 2008, **33**, 2921.

- [15] Y. Ren and L. Gao, *J. Am. Ceram. Soc.* 2010, **93**, 3560.
- [16] L. Feng, Y. Zhu, H. Ding and C. Ni, *J. Power Sources* 2014, **267**, 430.
- [17] S. I. Kim, J. S. Lee, H. J. Ahn, H. K. Song and J. H. Jang, *ACS Appl. Mater. Interfaces* 2013, **5**, 1596.
- [18] S. Ding, T. Zhu, J. S. Chen, Z. Wang, C. Yuan and X. W. Lou, *J. Mater. Chem.* 2011, **21**, 6602.
- [19] M. S. Wu, Y. A. Huang and C. H. Yang, *J. Electrochem. Soc.* 2008, **155**, A798.
- [20] C. Yuan, X. Zhang, L. Su, B. Gao and L. Shen, *J. Mater. Chem.* 2009, **19**, 5772.
- [21] B. Zhao, J. Song, P. Liu, W. Xu, T. Fang, Z. Jiao, H. Zhang and Y. Jiang, *J. Mater. Chem.* 2011, **21**, 18792.
- [22] S. T. Meek, J. A. Greathouse and M. D. Allendorf, *Adv. Mater.* 2011, **23**, 249.
- [23] K. E. deKrafft, C. Wang and W. Lin, *Adv. Mater.* 2012, **24**, 2014.
- [24] W. Cho, Y. H. Lee, H. J. Lee and M. Oh, *Adv. Mater.* 2011, **23**, 1720.
- [25] E. Ruiz, S. Alvarez, R. Hoffmann and J. Bernsteid, *J. Am. Chem. Soc.* 1994, **116**, 8206; R. Lu, Y. Chen, H. Zhou and A. Yuan, *Acta Chim. Sinica* 2010, **68**, 1199.
- [26] B. Wang, J. S. Chen, Z. Wang, S. Madhavi and X. W. Lou, *Adv. Energy Mater.* 2012, **2**, 1188.
- [27] Y. G. Wang and Y. Y. Xia, *Electrochim. Acta* 2006, **51**, 3223.
- [28] J. W. Lang, L. B. Kong, W. J. Wu, Y. C. Luo and L. Kang, *Chem. Commun.* 2008, 4213.
- [29] M. S. Wu, C. H. Yang and M. J. Wang, *Electrochim. Acta* 2008, **54**, 155.

2D nanoporous NiO nanosheets were synthesized from metal-organic frameworks as precursors using a facile method, which exhibited superior capacitive properties.

